Ultrasound-Assisted Selective Hydrogenation of C-5 Acetylene Alcohols with Lindlar Catalysts

B. Tripathi[a], L. Paniwnyk[a], N. Cherkasov[b], A.O. Ibhadon*[b], T. Lana-Villarreal[c], R. Gómez[c]

[a] Sonochemistry Centre, Department of Health and Life Sciences, Coventry University, James Starley Building, Priory Street, Coventry CV1 5FB, United Kingdom

[b] Catalysis and Reactor Engineering Research Group, Department of Chemistry and School of Biological Biomedical and Environmental Sciences, University of Hull, Cottingham Road, Hull HU6 7RX, United Kingdom

[c] Departament de Química Física i Institut Universitari d'Electroquímica, Universitat d'Alacant, Ap. 99, E-03080 Alicante, Spain

* Corresponding author: a.o.ibhadon@hull.ac.uk (A.O. Ibhadon), Tel: +44 1723 357318, Fax: +44 1723 370815

Abstract

The selective hydrogenation of 2-methyl-3-butyn-2-ol (MBY) was performed in the presence of Lindlar catalyst, comparing conventional stirring with sonication at different frequencies of 40, 380 and 850 kHz. Under conventional stirring, the reaction rates were limited by intrinsic kinetics, while in the case of sonication, the reaction rates were 50-90% slower. However, the apparent reaction rates were found to be significantly frequency dependent with the highest rate observed at 40 kHz. The original and the recovered catalysts after the hydrogenation reaction were compared using bulk elemental analysis, powder X-ray diffraction and scanning and transmission electron microscopy coupled with energy-dispersive X-ray analysis. The studies showed that sonication led to the frequency-dependent fracturing of polycrystalline support particles with the highest impact caused by 40 kHz sonication, while monocrystals were not damaged. In contrast, the leaching of Pd/Pb particles did not depend on the frequency, which suggests that sonication removed only loosely-bound catalyst particles.

Keywords

Ultrasound, Semihydrogenation, Lindlar catalyst, alkynol, palladium

1. Introduction

The liquid phase selective hydrogenation of alkynes to alkenes is an important reaction used in the synthesis of many vital chemicals. For example, the synthesis of vitamins A and E requires several selective hydrogenation steps; fragrances such as linalyl acetate, linalool, and dimethyloctenol are prepared using a combination of full and selective hydrogenation reactions with the worldwide production of up to 100,000 tons a year [1–3]. On a smaller scale, but with much wider range of substrates, the synthesis of many pharmaceuticals and food additives includes selective hydrogenation reactions [4]. The state-of-the-art industrial technology of selective hydrogenation is based on batch stirred reactors in the presence of a solvent and Pb-doped Pd (Lindlar) catalysts [1–4] . This approach provides high alkene selectivity, but suffers from a number of drawbacks such as low energy efficiency and difficult parameter optimisation which should be performed when changing the substrate molecule [3].

Flow microreactors have many advantages over batch reactors including high heat and mass transfer coefficients, higher energy efficiency and small reaction volume, which not only makes the handling of hydrogen safer but also simplifies the control of reaction parameters and process optimisation [5–8]. However, there are difficulties associated with the handling of solid catalysts in microfluidic systems, for example mass transfer limitations [9,10] and reactor clogging by catalyst particles [11,12]. These problems require an alternative method of catalyst treatment in a flow reactor and ultrasonic (US) irradiation is a particularly promising technology in this regard [13], because it has been reported to prevent clogging of microreactor channels [12], increase selectivity and activity of heterogeneously catalysed reactions [14–17].

The effect of US treatment on chemical reactions is closely associated with the phenomenon of cavitation - the rapid nucleation, formation and collapse of microbubbles in a liquid medium caused by the acoustic waves [18]. In the presence of a heterogeneous catalyst, adsorbed gas molecules act as the nuclei for cavitation microbubble formation at the solid surface. The collapse of this bubble in the liquid creates a void which is quickly filled by a rapid liquid jet flow, generates strong shear forces, scatters liquid into tiny droplets, fragments solid particles into fine powders, or modifies the surface of the heterogeneous catalyst [19]. Among these parameters, it is mainly the US frequency that governs the distribution of US energy [14].

Literature shows that most of the studies on the effect of US on chemical reactions were performed only at the US frequency of 20 kHz, where greater acoustic energy can be generated to induce chemical reactions [20–23]. The reaction rates also depend on frequency [14,24–27] because the duration of the cavitation cycle is inversely proportional to frequency [28]. High frequency leads to a rapid decay of acoustic energy in the liquid medium and does not favour the occurrence of active cavitation as the time for growth, radial motion and collapse of bubbles may be insufficient [19]. Moreover, the degassing rate increases for higher frequencies, being at 500 kHz 5 times as high as one at 20 kHz sonication [29]. However, the frequency effects can much more complex and non-linearly depend on frequency. There are several reports, where high frequency (>100 kHz) ultrasonic irradiation facilitates chemical reactions via the formation reactive species such as radicals [30–34].

Disselkamp et al. [16,17,23] studied the effects of sonication on 3-buten-1-ol hydrogenation catalysed by Pd black catalysts and demonstrated a drastic, 30-fold, increase in the hydrogenation rate of the reaction performed by sonication in comparison to conventional

stirring. However, the reaction conditions used in these studies are different from those used in the hydrogenation industry. Firstly, instead of Pd black, supported Pd and bimetallic Pd-Pb catalysts are used in industry. Secondly, water was used as a solvent in the studies [16,17], while low-polar organic solvents are usually used in industry [35]. Solvent may have played an essential role, because it was found that sonication increased the apparent reaction rates by reactivation of the deactivated catalytic surface [15,16,23]. However, catalyst deactivation is usually associated with the accumulation of carbonaceous species on the catalyst surface, which are soluble in low-polar solvents [36]. Therefore, the aim of the current work was to study the effect of sonication on selective hydrogenation of 2-methyl-3-butyn-2-ol in the frequency range of 40 to 850 kHz using low-polar methanol solvent. In order to keep reaction configurations and geometries similar indirect sonication was employed via the use of various frequency ultrasonic baths. The use of direct sonication employing an ultrasonic horn type system was not a focus of this study as the reaction rates would be expected to be different as a result of that variation.

2. Experimental Section

2.1. Calibration of Ultrasonic Devices

All US devices were calibrated by the standard calorimetric method [37] over three consecutive runs and average values of temperature rise were used to calculate the US power for each frequency. Output US power (P_{out}) was calculated according to equation (1), where ΔT is the temperature rise at Δt time, C_p and M are molar heat capacity and molar mass of the water, which was used as a US-conductive media.

$$P_{out} = \Delta T \, \Delta t^{-1} \, C_p \, M \qquad (1)$$

As the mixing efficiency directly depends on the power density (US output power normalised by the reaction volume) at a particular US frequency, US power density was calculated, Table 1, to ensure the comparability of the data for different frequencies. The conversion of US power to power density was also essential because the solution volume used in this study was different for the multi-frequency system (250 mL) compared with the 40 kHz bath (100 mL). A detailed study of ultrasonic power dissipation and power density calculations for similar US devices is reported elsewhere [38,39].

Table 1. Acoustic power for Ultrasonic devices at different frequencies.

US frequency (kHz)	Nominal US Power (W)	Output US Power (W)	US Power Density (W cm^{-3})
40	300	18.6	0.19
380	900	19.0	0.08
850	250	29.3	0.12

2.2. Catalytic Hydrogenation

The hydrogenation of MBY (Sigma-Aldrich, >99%) was performed on the Lindlar catalyst (Aldrich) under US treatment at various frequencies or stirring at room temperature (20^{o}C). In a typical US hydrogenation experiment, 100 mg Lindlar catalyst and 20 mL methanol (Aldrich, 99.9%) were transferred into a 100 mL three-neck flat-bottomed Quick-fit® reaction flask. The flask was connected to a water-cooled condenser and a custom-made single gas manifold system. Before the reaction, the flask was evacuated to remove air, purged first with nitrogen (BOC, >99.99%), followed by hydrogen (BOC, 99.995%). The reaction was started by adding 20 mmol of MBY, turning on the US source or magnetic (conventional) stirring, and introducing hydrogen at 50 mL min^{-1} at 1 bar above the reaction mixture.

The study at 40 kHz was performed in a US water bath (Langford Ultrasonic, Model 375TT). Heating of the water bath due to sonication was compensated by adding ice to keep the temperature at 20 ± 2 ˚C. Higher frequencies of 380 and 850 kHz were studied using a non-sweeping multi-frequency US reactor (Meinhardt Ultraschaltechnik) with an in-built water cooling system. Following the results of Disselkamp et al. [16,17,23], sonicated reactions were performed only under US treatment without conventional stirring. The catalysts recovered after the US-enhanced hydrogenations were referred to as L40, L380 and L850, depending on the US frequency. The reaction using magnetic stirring was performed on a hot plate at a stirring rate of 1100 rpm with a similar 3-neck round bottom Quick-fit® flask which was immersed in a water bath - the catalyst recovered is designated Lstir. Reactions performed at various stirring rates and catalyst masses demonstrated that the reaction was not mass-transfer limited under magnetic stirring. After 2.5 h, the reaction flask was flushed with nitrogen and the catalyst was

recovered from the reaction mixture by centrifuging, washed with methanol (2x20 mL), and then dried for 24 h at 120 ^{o}C. The composition of the reaction mixture was determined with a Shimadzu GC-2010 gas chromatograph equipped with a Stabilwax capillary column; 1-octanol (Aldrich, 99.9%) was used as an internal standard. All hydrogenation reactions were repeated three times in order to ensure the reproducibility of the results.

2.3. Elemental Analysis

Palladium and lead loss due to US treatment was investigated by elemental analysis of each solid catalyst prior to and after the hydrogenation reactions. Three different samples of each catalyst were prepared to calculate the analytical errors. In a typical analysis, 20 mg of solid catalyst was dissolved in 2.5 mL aqua regia, diluted with deionised water to a volume of 50 mL and analysed using Perkin Elmer Optima 5300 DV Optical Emission Spectrometer. The concentrations of Pd and Pb were determined using 5-point calibration graphs at the wavelengths of 340.5 nm and 283.3 nm, respectively.

2.4. Electron Microscopy

Scanning electron microscopy (SEM) study was performed using a Hitachi S3000N microscope equipped with an X-ray detector, Bruker X-Flash 30. The catalyst samples were transferred on an adhesive carbon film and studied using a variable pressure mode. The particle size distribution was studied using a Hitachi TM-1000 table top electron microscope. A small amount of catalyst powder was loaded on a conductive adhesive carbon film, 15-30 images were taken from various areas of the catalyst and the particle size distribution was obtained analysing 3000-7000 individual particles for each sample with the ImageJ software.

Transmission electron microscopy (TEM) study was performed using a JEOL JEM-2010 instrument equipped with an X-ray detector OXFORD INCA Energy TEM 100 for EDX microanalysis. The acquisition of the images was performed using a digital camera GATAN ORIUS SC600.

2.5. Powder X-ray diffraction

Powder X-ray diffraction (PXRD) measurements of the samples were performed using an Empyrean powder X-ray diffractometer, equipped with monochromatic Cu-Kα X-ray radiation

source and linear matrix detector, in the 2θ range of 10-80^{o}, step size of 0.026^{o} and acquisition time 150 s per step.

3. Results and Discussion

3.1. Selective Hydrogenation

The scheme of MBY hydrogenation is presented in Fig. 1. The reaction consists of stepwise addition of hydrogen molecules to MBY, forming MBE, which can further be hydrogenated to the full, non-selective hydrogenation product, MBA. Importantly, the highest alkene yield using the Lindlar catalyst is usually about 95-98% depending on the substrate molecule and the reaction conditions, so MBE is significantly hydrogenated to MBA only when almost all MBY is consumed [3,40,41].

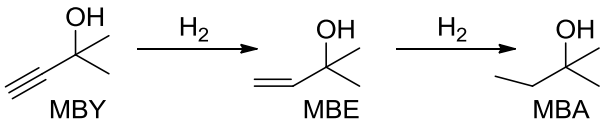

Fig. 1. Scheme of 2-methyl-3-butyn-2-ol (MBY) hydrogenation reactions using the Lindlar catalyst.

Table 2 presents the comparison of the hydrogenation performance of Lindlar catalyst under various reaction conditions. It is important to note that all catalysts were active under US treatment; however, the effect on the apparent reaction rates was frequency-dependent. The reaction performed with a conventional stirring provided the highest apparent reaction rate, while the reactions performed only under sonication showed an apparent reaction rate 2-10 times lower. Because the conventionally-stirred reaction was not mass-transfer limited, the lower apparent reaction rates observed under sonication indicate mass-transfer limitations. Interestingly, power dissipation during sonication was more than 50 times as high as during mechanical stirring, which shows that only a minor part of the energy was used for reactant mixing [42]. As a result of of mass transfer limitations, the apparent reaction rates were expected to depend on the US cavity geometry and other experimental parameters, but similar US power density dissipated during the reaction allows us to make valid qualitative conclusions regarding the effects of frequency. Sonication at 40 kHz provided the highest apparent reaction

rate thus the best catalyst / reagent mixing. A similar trend was observed by Carcenac et al. [43], where the surface cleaning effect reactivated the PtO_2 hydrogenation catalyst, resulting in improved mass transfer during the hydrogenation of (perfluoroalkyl) alkenes at 35 kHz. In the case of higher frequencies of 380 and 850 kHz, US mixing was relatively poor and this is reflected in lower MBY conversion. This can be attributed to the fact that during the mechanical agitation process, liquid convective motion is predominant in determining the rates of gas-liquid mass transfer compared with the liquid-phase turbulence predominant for the sonochemical processes [29]. Meanwhile, MBE selectivity at low alkyne conversion (<50 %) was above 98 %, which is typical for Lindlar catalyst [1-3], and did not depend on ultrasonic frequency showing the absence of internal diffusion limitations likely due to low porosity of the catalyst and high substrate concentration.

Table 2. The results of MBY hydrogenation after 2.5 h using conventional stirring (Lstir) and US treatment at different US frequencies of 40, 380, and 850 kHz (L40, L380, and L850, respectively). Reaction conditions: 100 mg Lindlar catalyst, 20 mmol MBY in 20 mL MeOH, at 20^{o}C and 1 bar H_2.

Catalyst	**Apparent reaction rate ($mmol_{MBY}$ h^{-1})**	**Initial MBE selectivity (%)**
Lstir	11.4	99.1
L40	5.1	99.2
L380	0.49	98.6
L850	1.9	98.2

To study the effect of US treatment on the catalysts, bulk metal content in the initial and recovered catalysts was compared. As shown in Fig. 2, the Pd and Pb content in the original Lindlar catalyst and the catalyst recovered after the hydrogenation reaction performed with the conventional stirring (Lstir) were very similar indicating no metal leaching from the catalyst after the reaction. These data agree with the good reusability of the Lindlar catalyst [3], which would have been impossible in the case of significant metal leaching.

On the other hand, the Pd and Pb metal content in all the US-treated catalysts was substantially lower than in the conventionally stirred catalyst, showing that sonication facilitated the removal of about 40% metal from the catalyst (Fig. 2). These data suggest that metal removal from the catalysts on sonication was taking place through fragmentation caused by the implosion of cavitation bubbles near the surface [44,45], possibly forming metallic nanoparticles, rather than leaching through the formation of soluble metal compounds. This data agrees well with the observations by Crespo-Quesada et al. [46], who noticed that supported Pd catalyst deactivated as a result of 15% leaching of active Pd after hydrogenation and US cleaning. Interestingly, the content of Pd and Pb in all US-treated catalysts was very similar, showing that metal removal from the catalyst surface was independent of US frequency, as only loosely-bound Pd-Pb particles were removed.

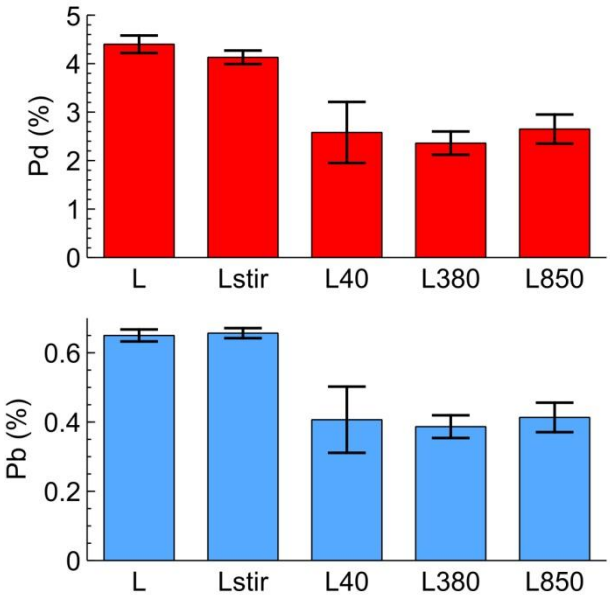

Fig. 2. Pd and Pb content (wt %) retained on the Lindlar catalysts after the hydrogenation for 2.5 h at 40, 380, 850 kHz US frequencies (L40, L380, L850, respectively), in comparison to the original Lindlar catalyst (L) and the catalyst after the reaction with the conventional stirring (Lstir).

3.3. The effect of US on the catalyst particles

Fig. 3 shows representative microphotographs of the Lindlar catalyst. The catalyst consists of polycrystalline $CaCO_3$ support particles 10-50 μm in diameter, which are built of crystallites of

about 5-20 μm (Fig. 3a). On the surface of the support, catalytically active Pd/Pb particles are very non-uniformly distributed, forming agglomerates up to 25 μm (Fig. 3b). TEM study (Fig. 3c), in agreement with SEM data, indicate that the original Lindlar catalyst surface is very heterogeneous.

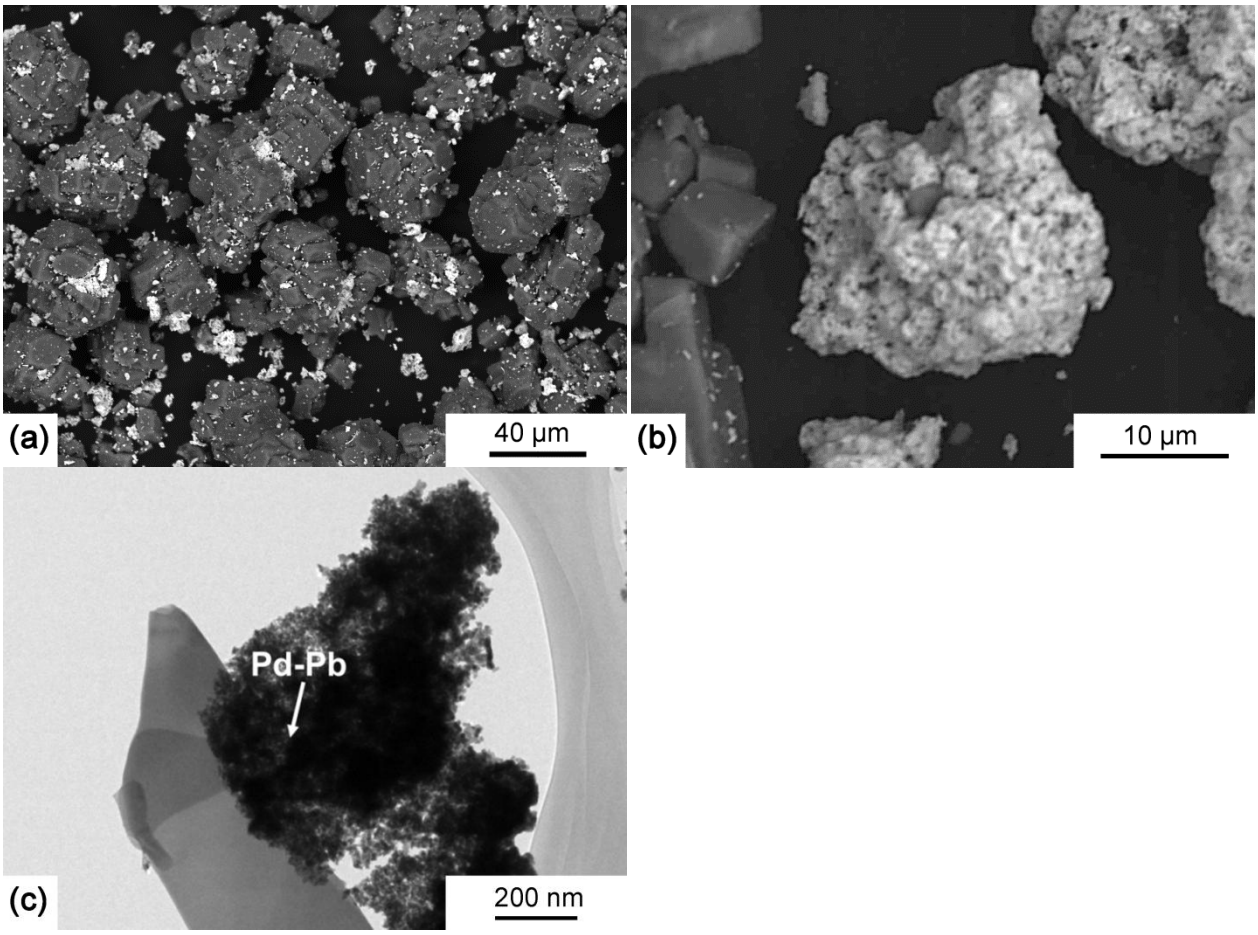

Fig. 3. (a, b) SEM and (c) TEM microphotographs of the Lindlar catalyst.

The catalyst used in hydrogenation under conventional stirring showed no alterations in the dimensions of the catalyst support particles. Catalytically active Pd/Pb particles were found in agglomerates 1-20 μm, as in the original Lindlar catalyst (Fig. 4a, b). On the other hand, in the US-treated catalyst L40, no agglomerates larger than 5 μm were found (Fig. 4c) demonstrating that sonication had a significant effect on the dimensions of the catalytically active Pd/Pb particles. Furthermore, TEM study of the L40 catalyst (Fig. 4d), show that some Pd/Pb particles were detached from the support material consistent with the observed decrease in Pd/Pb content in the sonicated catalysts (Fig. 2). Local EDX elemental analysis performed on different regions of the catalyst during the TEM study showed non-uniformity of elemental distribution

with the Pd/Pb mass ratio varying from 4:1 to 7:1, the ratio which agrees with the bulk Pd/Pb content (Fig. 2). The effects observed are attributed to interparticle collisions during the acoustic cavitation, which split and disperse the catalyst particles [47,48]. Bianci et al. [49], similarly, noticed some degeneration of the Pd/Al_2O_3 catalyst on sonication at 20 kHz, which created surface defects that dispersed the metal particles on the support at a given US frequency.

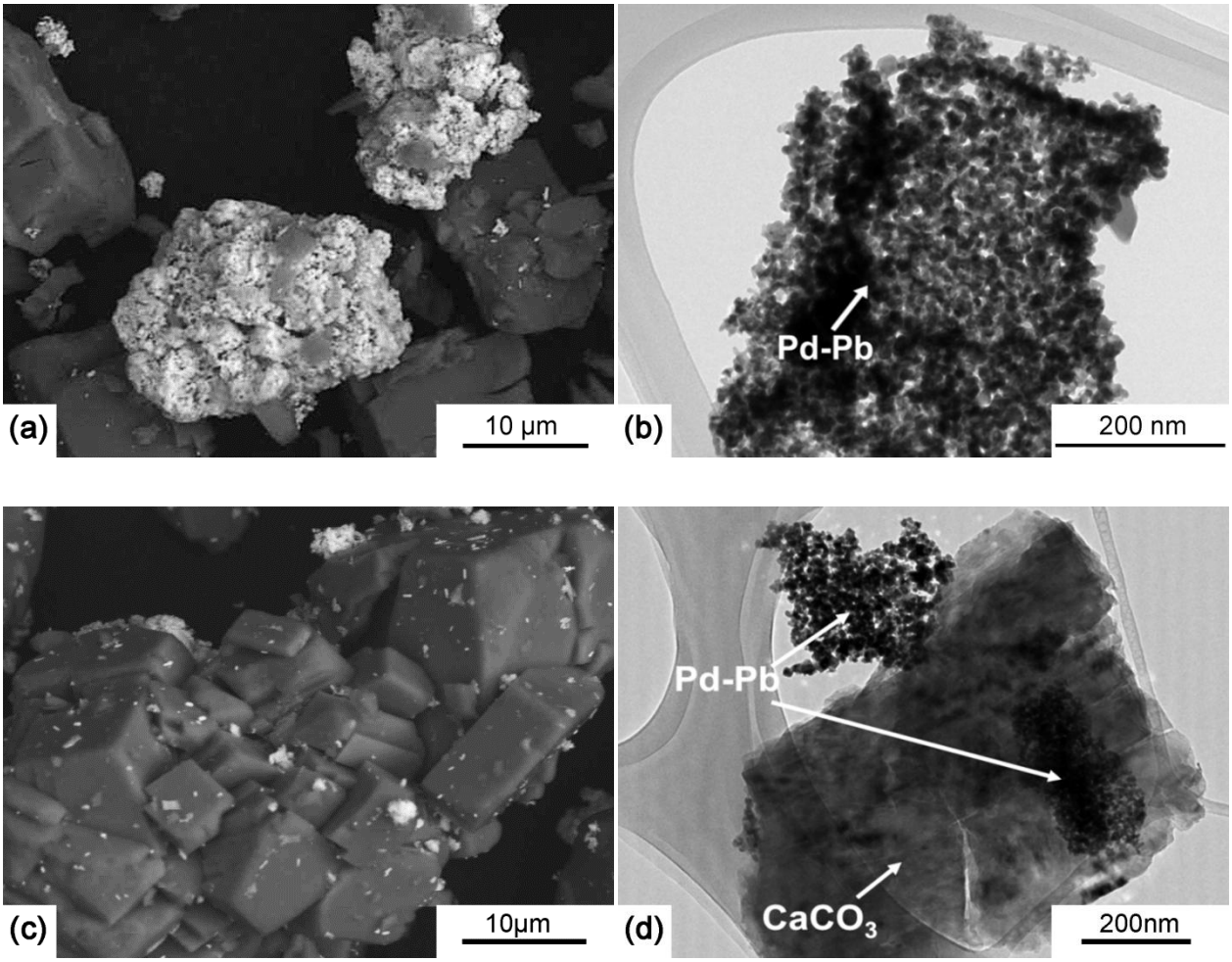

Fig.4. Representative SEM and TEM microphotographs of the (a, b) Lstir catalyst used in the hydrogenation with the conventional stirring, and (c, d) L40 US-treated catalyst at 40 kHz. Pd-Pb particles on TEM study were confirmed by EDX analysis.

Statistical analysis of the catalyst support after US treatment performed by studying 3000-7000 individual particles is presented in Fig. 5. The original Lindlar catalyst showed bimodal particle distribution with the most probable particle diameters of about 10 and 55 μm (Fig. 5a), which represent the particles of polycrystalline and monocrystalline $CaCO_3$ (Fig. 3). In contrast to the

original catalyst, L40 showed prevalence of 10-30 μm particles (Fig. 5b), clearly indicating the fracturing on sonication. The catalysts treated at higher US frequencies showed very similar particle distributions – the fraction of monocrystalline particles increased twofold in comparison with the original catalysts (Fig. 5c-d). However, the fracturing effect of US was much lower at the frequencies of 380 and 850 kHz compared to 40 kHz, probably due to much lower cavitation energy at higher US frequencies because of the shorter duration of acoustic cycles at higher frequencies [28,50].

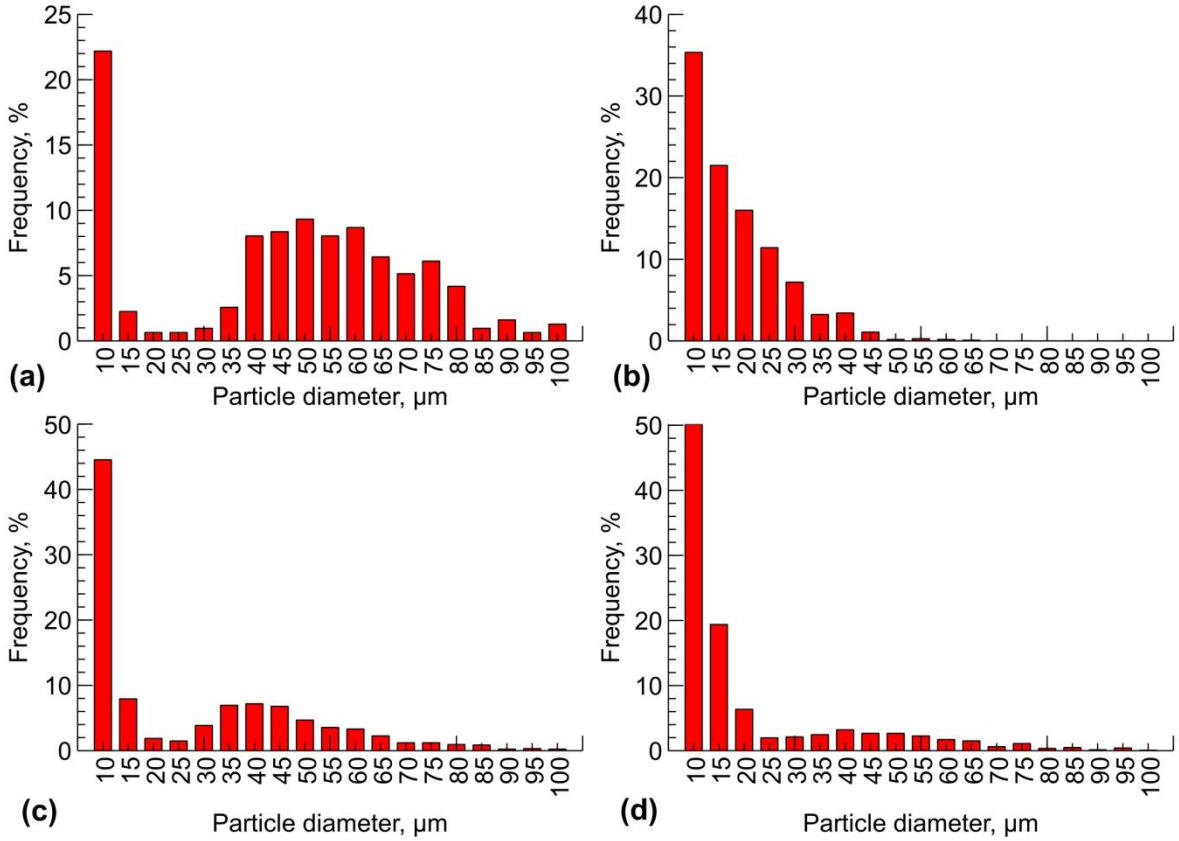

Fig. 5. Particle size distributions of (a) original Lindlar and catalysts (b) L40, (c) L380, (d) L850, treated at 40 kHz, 380 kHz and 850 kHz, respectively.

Fig. 6a presents a typical PXRD pattern of the original Lindlar catalyst. The pattern is dominated by strong and narrow reflexes corresponding to crystalline $CaCO_3$ catalyst support. However, a lower intensity and wider peak at about 40^o corresponds to the supported Pd particles. The magnified area of the studied catalysts at 2θ near 40^o is presented in Fig. 6b. High-intensity diffraction peaks at 39.5^o, which corresponds to $CaCO_3$, have the same width, demonstrating that US-treatment did not fracture significantly $CaCO_3$ monocrystals of the support material and

agrees with the SEM data. Similarly, low-intensity diffraction peak at 40.1^{o} has a very similar width for all the catalysts, showing that the dimensions of Pd crystallites did not change on US treatment. Size estimations of the Pd particles performed using the Scherrer equation showed a marginal decrease in the Pd crystallite size for the sonicated powder samples (8.7 – 8.2 nm, respectively) in comparison to the original Lindlar catalyst (9.7 nm). These results show that individual Pd crystallites were not fractured on US treatment. As a result, it may be concluded that the observed removal of Pd and Pb metals from the catalysts after US treatment (Fig. 2) was caused by the fragmentation of Pd/Pb polycrystals or the removal of the monocrystals from the surface of the support. The de-agglomeration of metal clusters was likely caused by the high velocity inter-particle collisions produced on cavitation [51,52].

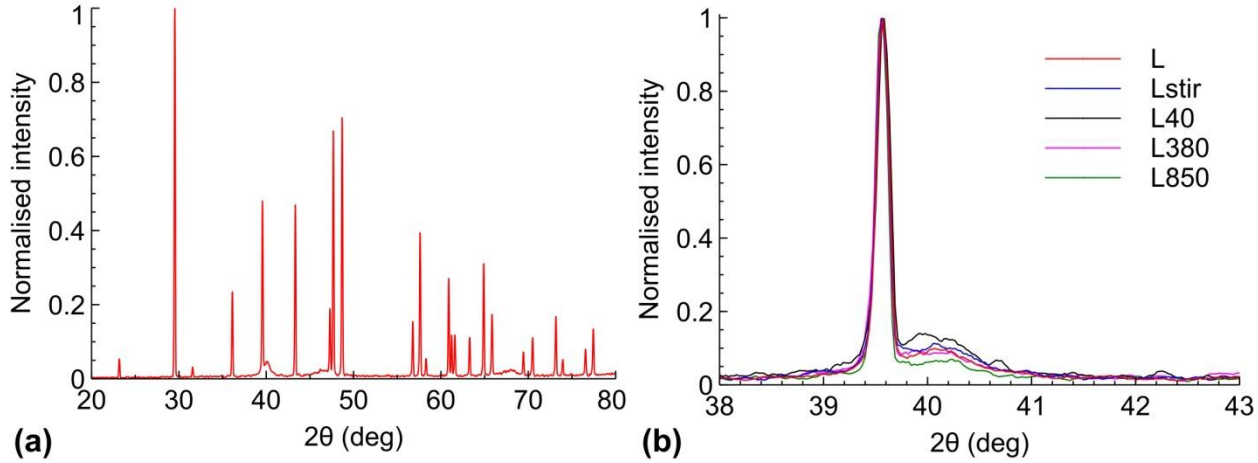

Fig. 6. PXRD patterns of (a) original Lindlar catalyst and (b) magnified area near 2θ= 40^{o} for all the studied catalysts.

5. Conclusions

The comparison of original and sonicated Lindlar catalysts as undertaken in this study was challenging due to the non-uniform distribution of Pd/Pb active particles on the catalyst surface. The combination of electron microscopy and X-ray diffraction studies showed that sonication significantly decreased the dimensions of $CaCO_3$ catalyst support particles, fracturing the polycrystals into monocrystals. Low US frequency of 40 kHz had the highest impact on the catalyst dimensions possibly due to the higher cavitation energy. The same effect was observed for catalytically active Pd/Pb particles that led to the leaching of about 40% of the Pd content from the catalyst, for all studied US frequencies. However, in this case the leaching was

frequency independent indicating that only loosely-bound Pd/Pb particles were removed under US treatment.

The comparison of MBY hydrogenation under sonication and conventional stirring showed that sonication alone cannot provide sufficient external mass transfer in a bulk batch chemical reactor. Mechanical stirring seems to be better for enhancing mass transfer than US, but for the apparent reaction rates under sonication were the highest for 40 kHz sonication.

Acknowledgements

Financial support from the EU commission for the MAPSYN project is greatly acknowledged (MAPSYN.eu No. CP-IP 309376). The authors thank Steve Allitt for preliminary SEM imaging at Coventry University; Dr. C. Wilies, Professor B. Binks and Professor P. Fletcher at the University of Hull for the access to their equipment and S. Johnston for SEM analysis of Lindlar catalysts.

References

[1] M. Eggersdorfer, D. Laudert, U. Létinois, T. McClymont, J. Medlock, T. Netscher, W. Bonrath, Angew. Chemie Int. Ed. 51 (2012) 12960–12990.

[2] W. Bonrath, M. Eggersdorfer, T. Netscher, Catal. Today 121 (2007) 45–57.

[3] W. Bonrath, J. Medlock, J. Schutz, B. Wüstenberg, T. Netscher, Hydrogenation in the Vitamins and Fine Chemicals Industry – An Overview, In: I. Karame (Ed.) Hydrogenation, InTech, Rijeka, 2012, Pp. 69-90., InTech, 2012.

[4] B. Chen, U. Dingerdissen, J.G.E. Krauter, H.G.J. Lansink Rotgerink, K. Möbus, D.J. Ostgard, P. Panster, T.H. Riermeier, S. Seebald, T. Tacke, H. Trauthwein, Appl. Catal. A Gen. 280 (2005) 17–46.

[5] Z. Wu, E. Borretto, J. Medlock, W. Bonrath, G. Cravotto, ChemCatChem 6 (2014) 2762–2783.

[6] V. Hessel, G. Cravotto, P. Fitzpatrick, B.S. Patil, J. Lang, W. Bonrath, Chem. Eng. Process. Process Intensif. 71 (2013) 19–30.

[7] R.A. Skilton, A.J. Parrott, M.W. George, M. Poliakoff, R.A. Bourne, Appl. Spectrosc. 67 (2013) 1127–31.

[8] K. Jähnisch, V. Hessel, H. Löwe, M. Baerns, Angew. Chemie Int. Ed. 43 (2004) 406–46.

[9] B.H. Alsolami, R.J. Berger, M. Makkee, J.A. Moulijn, Ind. Eng. Chem. Res. 52 (2013) 9069–9085.

[10] D. van Herk, P. Castaño, M. Makkee, J.A. Moulijn, M.T. Kreutzer, Appl. Catal. A Gen. 365 (2009) 199–206.

[11] L.N. Protasova, M. Bulut, D. Ormerod, A. Buekenhoudt, J. Berton, C. V. Stevens, Org. Process Res. Dev. 17 (2013) 760–791.

[12] T. Noël, J.R. Naber, R.L. Hartman, J.P. McMullen, K.F. Jensen, S.L. Buchwald, Chem. Sci. 2 (2011) 287–290.

[13] Z. Dong, C. Yao, X. Zhang, J. Xu, G. Chen, Y. Zhao, Q. Yuan, Lab Chip 15 (2015) 1145–1152.

[14] T.J. Mason, D. Peters, Practical Sonochemistry: Power Ultrasound Uses and Applications, Elsevier Science, 2002.

[15] T.J. Mason, J.P. Lorimer, L. Paniwnyk, P.W. Wright, A.R. Harris, J. Catal. 147 (1994) 1–4.

[16] R.S. Disselkamp, Y.-H. Chin, C.H.F. Peden, J. Catal. 227 (2004) 552–555.

[17] R.S. Disselkamp, K.M. Judd, T.R. Hart, C.H.F. Peden, G.J. Posakony, L.J. Bond, J. Catal. 221 (2004) 347–353.

[18] G. Cravotto, P. Cintas, Chem. Soc. Rev. 35 (2006) 180–96.

[19] J. Luo, Z. Fang, R.L. Smith, Prog. Energy Combust. Sci. 41 (2014) 56–93.

[20] S. Merouani, O. Hamdaoui, F. Saoudi, M. Chiha, Chem. Eng. J. 158 (2010) 550–557.

[21] Z. Yang, S. Matsumoto, H. Goto, M. Matsumoto, R. Maeda, Sensors Actuators A Phys. 93 (2001) 266–272.

[22] Tandiono, S.-W. Ohl, D.S.W. Ow, E. Klaseboer, V. V Wong, R. Dumke, C.-D. Ohl, Proc. Natl. Acad. Sci. U. S. A. 108 (2011) 5996–8.

[23] R.S. Disselkamp, K.M. Denslow, T.R. Hart, J.F. White, C.H.F. Peden, Appl. Catal. A Gen. 288 (2005) 62–66.

[24] C. Petrier, M.F. Lamy, A. Francony, A. Benahcene, B. David, V. Renaudin, N. Gondrexon, J. Phys. Chem. 98 (1994) 10514–10520.

[25] B.P. Mason, K.E. Price, J.L. Steinbacher, A.R. Bogdan, D.T. McQuade, Chem. Rev. 107 (2007) 2300–18.

[26] D. Chen, S.K. Sharma, A. Mudhoo, Handbook on Applications of Ultrasound: Sonochemistry for Sustainability, CRC Press, 2011.

[27] T.Y. Wu, N. Guo, C.Y. Teh, J.X.W. Hay, Advances in Ultrasound Technology for Environmental Remediation, Springer Science & Business Media, 2012.

[28] L.H. Thompson, L.K. Doraiswamy, Ind. Eng. Chem. Res. 38 (1999) 1215–1249.

[29] A. Kumar, P.R. Gogate, A.B. Pandit, H. Delmas, A.M. Wilhelm, Ind. Eng. Chem. Res. 43 (2004) 1812–1819.

[30] C. Petrier, A. Jeunet, J.-L. Luche, G. Reverdy, J. Am. Chem. Soc. 114 (1992) 3148–3150.

[31] J. Wang, M. Pelletier, H. Zhang, H. Xia, Y. Zhao, Langmuir 25 (2009) 13201–13205.

[32] V. Renaudin, N. Gondrexon, P. Boldo, C. Pétrier, a. Bernis, Y. Gonthier, Ultrason. Sonochem. 1 (1994) S81–S85.

[33] I.D. Manariotis, H.K. Karapanagioti, C. V Chrysikopoulos, Water Res. 45 (2011) 2587–2594.

[34] T.J. Mason, Ultrason. Sonochem. 14 (2007) 476–483.

[35] W. Bonrath, B. Heller, Reacting bis(3-Rsubstituted -2-Propynyl)ether with Acetonitrile in Presence of a Cobalt Complex Catalystl, US 10/490,196, 2004.

[36] Á. Molnár, A. Sárkány, M. Varga, J. Mol. Catal. A Chem. 173 (2001) 185–221.

[37] J.P. Lorimer, T.J. Mason, Chem. Soc. Rev. 16 (1987) 239–274.

[38] M. Dükkancı, M. Vinatoru, T.J. Mason, Ultrason. Sonochem. 21 (2014) 846–853.

[39] M. Dükkancı, M. Vinatoru, T.J. Mason, J. Adv. Oxid. Technol. 15 (2012) 277–283.

[40] F. Liguori, P. Barbaro, J. Catal. 311 (2014) 212–220.

[41] M.P. Spee, J. Boersma, M.D. Meijer, M.Q. Slagt, G. van Koten, J.W. Geus, J. Org. Chem. 66 (2001) 1647–1656.

[42] J. Hajek, D.Y. Murzin, Ind. Eng. Chem. Res. 43 (2004) 2030–2038.

[43] Y. Carcenac, M. Tordeux, C. Wakselman, P. Diter, J. Fluor. Chem. 126 (2005) 1347–1355.

[44] W. Lauterborn, W. Hentschel, Ultrasonics 24 (1986) 59–65.

[45] F. Ali, L. Reinert, J.-M. Levêque, L. Duclaux, F. Muller, S. Saeed, S.S. Shah, Ultrason. Sonochem. 21 (2014) 1002–1009.

[46] M. Crespo-Quesada, M. Grasemann, N. Semagina, A. Renken, L. Kiwi-Minsker, Catal. Today 147 (2009) 247–254.

[47] K.S. Suslick, Science 247 (1990) 1439–1445.

[48] E.A. Neppiras, Ultrasonics 22 (1984) 25–28.

[49] C. Bianchi, R. Carli, S. Lanzani, D. Lorenzetti, G. Vergani, V. Ragaini, Ultrason. Sonochem. 1 (1994) S47–S49.

[50] M. Lim, Y. Son, J. Khim, Ultrason. Sonochem. 18 (2011) 460–265.

[51] A. Nemamcha, J.L. Rehspringer, Rev. Adv. Mater. Sci. 18 (2008) 685–688.

[52] S.F. Moya, R.L. Martins, A. Ota, E.L. Kunkes, M. Behrens, M. Schmal, Appl. Catal. A Gen. 411-412 (2012) 105–113.